isvr Institute of Sound and Vibration Research

Active Control of the Flexural Vibration of a Thin Beam with Free Ends

M.R. Dench, M.J. Brennan and N.S. Ferguson

ISVR Technical Memorandum No 949

July 2005

University of Southampton

SCIENTIFIC PUBLICATIONS BY THE ISVR

Technical Reports are published to promote timely dissemination of research results by ISVR personnel. This medium permits more detailed presentation than is usually acceptable for scientific journals. Responsibility for both the content and any opinions expressed rests entirely with the author(s).

Technical Memoranda are produced to enable the early or preliminary release of information by ISVR personnel where such release is deemed to the appropriate. Information contained in these memoranda may be incomplete, or form part of a continuing programme; this should be borne in mind when using or quoting from these documents.

Contract Reports are produced to record the results of scientific work carried out for sponsors, under contract. The ISVR treats these reports as confidential to sponsors and does not make them available for general circulation. Individual sponsors may, however, authorize subsequent release of the material.

UNIVERSITY OF SOUTHAMPTON

INSTITUTE OF SOUND AND VIBRATION RESEARCH

DYNAMICS GROUP

Active Control of the Flexural Vibration of a Thin Beam with Free Ends

by

M.R. Dench, M.J. Brennan and N.S. Ferguson

ISVR Technical Memorandum No: 949

July 2005

Authorised for issue by
Professor M.J. Brennan
Group Chairman

Abstract

This report presents the theory and computer simulations for the active control of the kinetic energy of a thin beam with free ends driven by a single harmonic primary point force by using a single secondary point force. A beam with free ends has two rigid body modes corresponding to translation and rotation of the beam without bending. Models were developed using two methodologies to calculate the total time averaged kinetic energy of the beam. The first considers the beam as a continuous elastic structure. The second considers the beam as a series of lumped masses and sums the kinetic energy of each small mass element. The results from both methods agree if the number of small mass elements per wavelength in the discrete model is greater than 5. By formulating the models using the standard Hermitian quadratic form, one can use existing methods for minimising the total time averaged kinetic energy of the beam. Numerical examples are given for the optimum magnitude and phase of a single secondary force for a single primary force. The results show that a large proportion of the total kinetic energy of the beam can be attributed to energy in the rigid body modes for frequencies well below the first flexural mode. This suggests that a simple control strategy would be to minimise the kinetic energy in the rigid body modes. A simple model was thus developed to minimise the kinetic energy in the two rigid body modes. Using this latter model is was possible to determine how effective a secondary force would be in reducing the overall kinetic energy by considering the relative positions of the two forces. The optimum position for the secondary force is always co-located with the primary force. In which case, total cancellation can be achieved if the secondary force is of the same magnitude and 180 degrees out of phase, as expected.

Table of Contents

1 Introduction

There are many reasons why it may be desirable to reduce vibration levels within a structure. For example, excessive vibration may accelerate fatigue failure of the structure itself. Reducing the vibration levels may make the structure more inhabitable for persons or equipment and may reduce the sound radiated by the structure. Machinery areas on mobile platforms such as ships often consist of several machines mounted on the same elastic raft. In order to reduce the vibration due to unbalance in rotating or reciprocating machinery the raft is then isolated from the hull structure by compliant mounts as shown in figure 1.1.

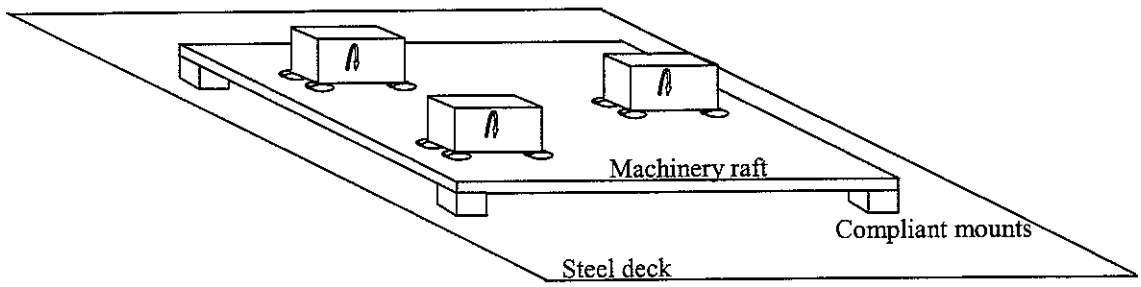

Figure 1.1 Rotating machinery on an elastic machinery raft with vibration isolating mounts between the machines and the raft and between the raft and the steel deck.

These mounts are essentially damped springs and may not be effective at all frequencies at which vibrations are occurring. Passive control, by the addition of mass, damping materials or vibration neutralisers may be employed to reduce vibration. Active control is achievable by electromagnetic levitation of the machinery – active rafting, active damping of residual vibration or active vibration control. Several approaches to active vibration control are possible (Brennan *et al,* 1995*)*, including a wave control approach (Halkyard and Mace, 2002) and energy control. Energy may be minimised by means of either piezoelectric actuators applying secondary moments to the structure (Gaudenzi *et al*, 2000; Di Turo, 2003) or force actuators applying controlling forces to the structure.

The broad aim of this research is to study the interactions between these multiple vibrating systems when mounted on a common elastic structure, and to study how the structure vibrates:

1. When the systems are driven by a common power supply.
2. When the systems operate under different loading conditions.
3. With various masses attached to the elastic structure.
4. With Active Control Techniques applied to the structure.

This report addresses the first and last point. The positioning of the machines is likely to be determined by engineering factors other than vibration control. Since the machines are driven by a common power supply, this report investigates the possibility of minimising the kinetic energy transmitted to the machinery raft by controlling the phase of the power supplied to each machine. This process known as synchrophasing is well documented for controlling aircraft propeller and duct fan noise (Risi *et al*, 1996). In order to simplify the problem, the machinery raft will be modelled as a thin beam with free ends. Machinery on the raft will be represented by point forces. In this report only two point forces are considered, however the general theory is developed for more than one secondary point force.

The aim of this report is to present the theory and computer simulations for the active control of the kinetic energy of a thin beam driven by a single harmonic primary point force by using a single secondary point force. This method is easily adaptable to a higher level of active control by using more secondary forces (Nelson and Elliott, 1992). This report will form the basis for an experimental investigation which will follow.

2 Development of a model

2.1 Simplifications

In order to simplify the problem, the dynamic system is represented by either one or two point forces acting on a thin elastic beam. Figure 2.1 shows the right handed coordinate system used to represent the lateral vibration $w(x,t)$ of a beam of length l and the positions x_1 and x_2 of any applied forces f_1 and f_2.

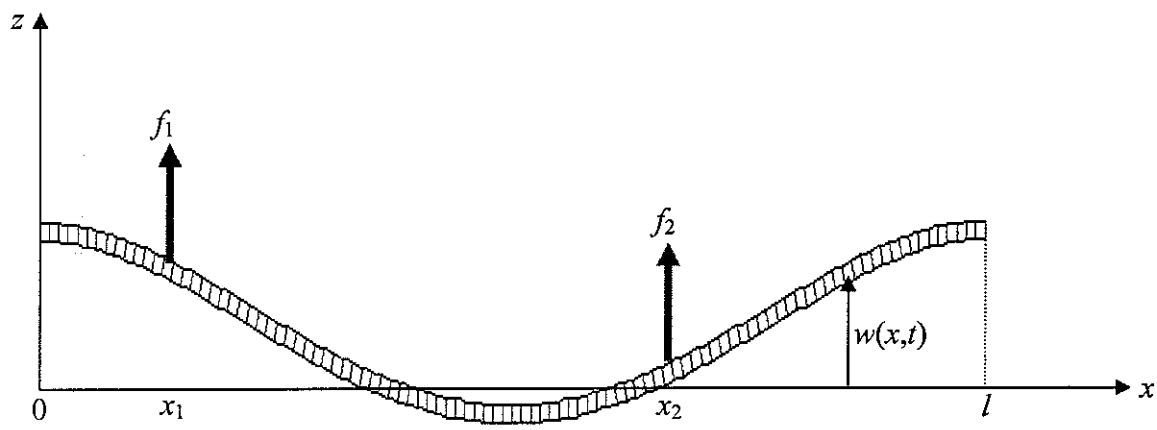

Figure 2.1 Coordinate system and variables used in modelling the lateral vibration of a thin beam.

When the wavelength of the flexural wave is large compared to the thickness of the elastic beam, the effects of shear deformation and rotary inertia can be ignored, leading to the simple Euler-Bernoulli beam theory (Warburton, 1976). The ends of the beam are assumed to have free boundary conditions. The reasons for considering a beam with free ends are that

1. It is possible to validate the theory for a beam with free end conditions at high frequencies by empirical measurements on a finite length beam with ends supported by rubber mounts.

2. It is possible to model the effects of linear springs and dampers connected to the ends of the beam by changing the equations for the shear force and to model the effects of end connected torsional springs and dampers by modifying the equations for the bending moment.

2.2 Free lateral vibration of a thin beam with free ends

Euler-Bernoulli thin beam theory gives the equation of motion for the free lateral vibration of a uniform thin beam as (Rao,2004)

$$EI\frac{\partial^4 w(x,t)}{\partial x^4}+\rho A\frac{\partial^2 w(x,t)}{\partial t^2}=0 \tag{2.1}$$

where E is the Young's modulus, I is the moment of inertia of the beam cross section about the neutral axis (the y axis in figure 1.1), ρ is the density and A is the cross sectional area of the beam. Assuming a time harmonic solution of the form $w(x,t)=\phi(x)\, e^{j\omega t}$ and using the method of separation of variables the general solution is given by (Rao, 2004).

$$w(x,t)=(C_1\cos\beta x+ C_2\sin\beta x+ C_3\cosh\beta x+ C_4\sinh\beta x)\, e^{j\omega t} \tag{2.2}$$

where C_1, C_2, C_3 and C_4 are constants determined by the boundary conditions and $\beta=\sqrt{\frac{\omega}{c}}$ is the flexural wavenumber, with the flexural wavespeed $c=\sqrt{\frac{EI}{\rho A}}$

The free end boundary conditions are:

$$\text{bending moment } M=EI\frac{\partial^2 w(x,t)}{\partial x^2}=0 \text{ at } x=0 \text{ and } x=l \tag{2.3}$$

$$\text{shear force } S=EI\frac{\partial^3 w(x,t)}{\partial x^3}=0 \text{ at } x=0 \text{ and } x=l \tag{2.4}$$

Equations 2.3 and 2.4 evaluated at $x=0$ results in $C_3=C_1$ and $C_4=C_2$.
The boundary conditions at $x=l$ lead to the equation:

$$\begin{bmatrix}\cosh\beta l-\cos\beta l & \sinh\beta l-\sin\beta l\\ \sin\beta l+\sinh\beta l & \cosh\beta l-\cos\beta l\end{bmatrix}\begin{bmatrix}C_1\\ C_2\end{bmatrix}=\begin{bmatrix}0\\ 0\end{bmatrix} \tag{2.5}$$

For non-trivial solutions

$$\begin{vmatrix}\cosh\beta l-\cos\beta l & \sinh\beta l-\sin\beta l\\ \sin\beta l+\sinh\beta l & \cosh\beta l-\cos\beta l\end{vmatrix}=0$$

which leads to the characteristic equation:

$$\cos \beta l \cosh \beta l = 1 \tag{2.6}$$

The roots of equation 2.6 correspond to the natural frequencies of vibration of the beam with free ends. Equation 2.6 cannot be solved analytically, but values for βl can be found by using a mathematical package such as MATLAB. The n^{th} natural frequency is given by (Rao, 2004)

$$\omega_n = (\beta_n l)^2 \sqrt{\frac{EI}{\rho A l^4}} \tag{2.7}$$

where

$\beta_0 l$	$\beta_1 l$	$\beta_2 l$	$\beta_3 l$	$\beta_n l$
0 For two rigid body modes	4.730041	7.853205	10.995608	$\approx (n+\frac{1}{2})\pi$

Using equation 2.2 to obtain $\frac{\partial^2 w(x,t)}{\partial x^2}$ evaluated at the boundary $x=l$ gives

$$C_1 = C_2 \frac{(\sin \beta_n l - \sinh \beta_n l)}{(\cosh \beta_n l - \cos \beta_n l)}$$

Hence the n^{th} modeshape is given by

$$\phi_n(x) = \sin \beta_n x + \sinh \beta_n x + \alpha_n (\cos \beta_n x + \cosh \beta_n x)$$

where $\alpha_n = \frac{(\sin \beta_n l - \sinh \beta_n l)}{(\cosh \beta_n l - \cos \beta_n l)}$

Figure 2.2 shows the first few modeshapes of a thin Euler-Bernoulli beam with free ends. Two rigid body modes exist for a thin beam with free ends, these correspond to pure translation and rotation of the beam without bending.

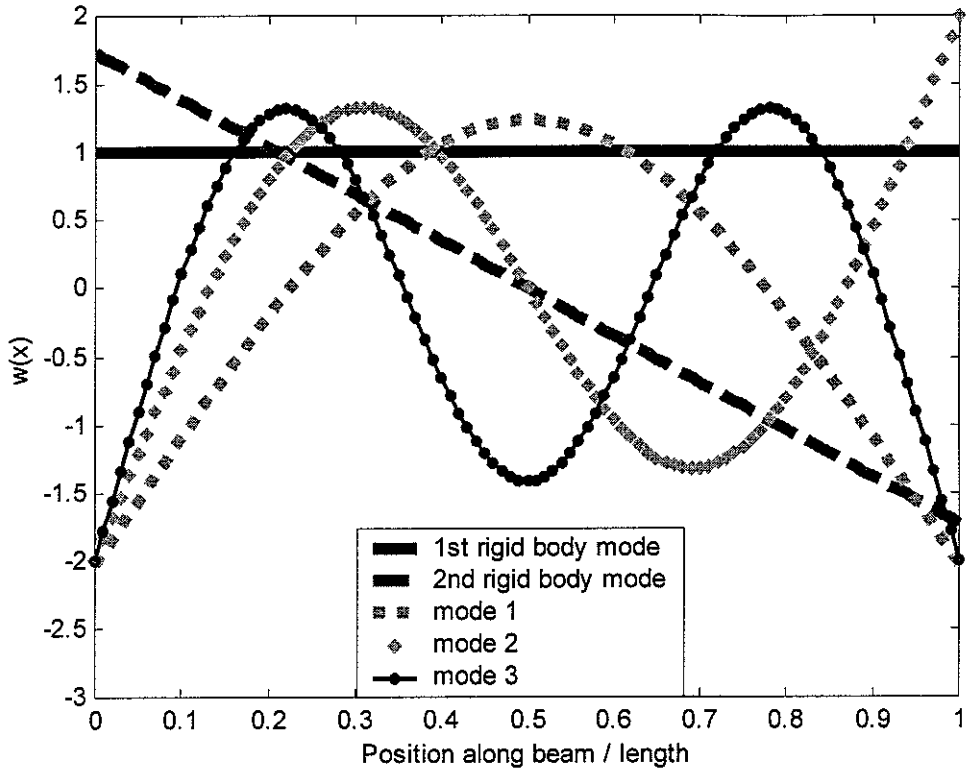

Figure 2.2 Rigid body modes and first 3 flexible modeshapes of a thin beam with free ends

It is also shown (Rao 2004; Warburton 1976) that the modeshapes of the uniform beam are orthogonal, which means that

$$\int_0^l \phi_m(x)\phi_n(x)dx = 0 \text{ for } m \neq n \tag{2.8}$$

The orthogonality condition means that the energy in each mode does not leak into any of the other modes. This leads to the equation for the general vibration of a free beam as the sum of the modal basis functions given by

$$w(x,t) = \sum_{n=0}^{\infty} \phi_n(x) q_n(t) \tag{2.9}$$

Where ϕ_n is the modeshape of the n^{th} mode at x and q_n is the modal amplitude, i.e. how much of each mode is present in the general vibration. This is discussed further in the next section.

2.3 Forced lateral vibration of a thin beam with free ends

The equation of motion for the forced lateral vibration of a uniform thin beam is given by

$$EI\frac{\partial^4 w(x,t)}{\partial x^4}+\rho A\frac{\partial^2 w(x,t)}{\partial t^2}=f(x,t) \tag{2.10}$$

where $f(x,t)$ is an external force per unit length. Using equation (2.9) the lateral vibration of the forced beam can be described by a modal superposition. Equation (2.9) can be differentiated to give

$$\frac{\partial^4 w(x,t)}{\partial x^4}=\sum_{n=0}^{\infty}\frac{d^4\phi_n(x)}{dx^4}q_n(t) \quad \text{and} \quad \frac{\partial^2 w(x,t)}{\partial t^2}=\sum_{n=0}^{\infty}\phi_n(x)\frac{d^2 q_n(t)}{dt^2}$$

These can be substituted into equation (2.10) to give

$$EI\sum_{n=0}^{\infty}\frac{d^4\phi_n(x)}{dx^4}q_n(t)+\rho A\sum_{n=0}^{\infty}\frac{d^2 q_n(t)}{dt^2}\phi_n(x)=f(x,t) \tag{2.11}$$

Assuming a time harmonic point force at $x = x_1$ of the form $f(x,t)=f\,\delta(x-x_1)\,e^{j\omega t}$ the steady state response is given by

$$w(x,t)=\sum_{n=0}^{\infty}\phi_n(x)q_n(t)=\sum_{n=0}^{\infty}\frac{\phi_n(x)\phi_n(x_1)}{m_n(\omega_n^2(1+j\eta)-\omega^2)}f(x_1)e^{j\omega t} \tag{2.12}$$

where proportional damping has been included via a constant modal structural loss factor η and m_n is the modal mass. The transfer receptance due to a harmonic force applied at x_1 is given by

$$\frac{w(x)}{f(x_1)}=\sum_{n=0}^{\infty}\frac{\phi_n(x)\phi_n(x_1)}{m_n(\omega_n^2(1+j\eta)-\omega^2)}$$ which can be written as

$$\frac{w(x)}{f(x_1)}=\left(\frac{1}{-m\omega^2}+\frac{3}{-m\omega^2}\left(1-\frac{2x}{l}\right)\left(1-\frac{2x_1}{l}\right)+\sum_{n=1}^{\infty}\frac{\phi_n(x)\phi_n(x_1)}{m_n(\omega_n^2(1+j\eta)-\omega^2)}\right) \tag{2.13}$$

where m is the mass of the beam. The first two terms are due to the rigid body motion of the beam with two free ends, corresponding to modeshapes $\phi(x)=1$ and $\phi(x)=\sqrt{3}\left(1-\frac{2x}{l}\right)$ (Gardonio and Brennan, 2004).

Figure 2.3 shows the point accelerance $\frac{\ddot{w}(x,t)}{f(x,t)} = -\omega^2 \frac{w(x)}{f(x)}$ for a uniform rectangular cross section steel beam of length 2m and thickness 2cm, with a point force applied in the centre. A proportional damping of 10% (η=0.1) has been used. This is compared to the driving point accelerance of an infinite beam given by (Gardonio and Brennan, 2004)

$$\frac{\ddot{w}_\infty}{f} = \omega^2 \frac{(1+j)}{4EI\beta^3} \tag{2.14}$$

and the low frequency result where only the translational rigid body mode is excited. In this low frequency case $\frac{\ddot{w}_{lf}}{f} = \frac{1}{m}$.

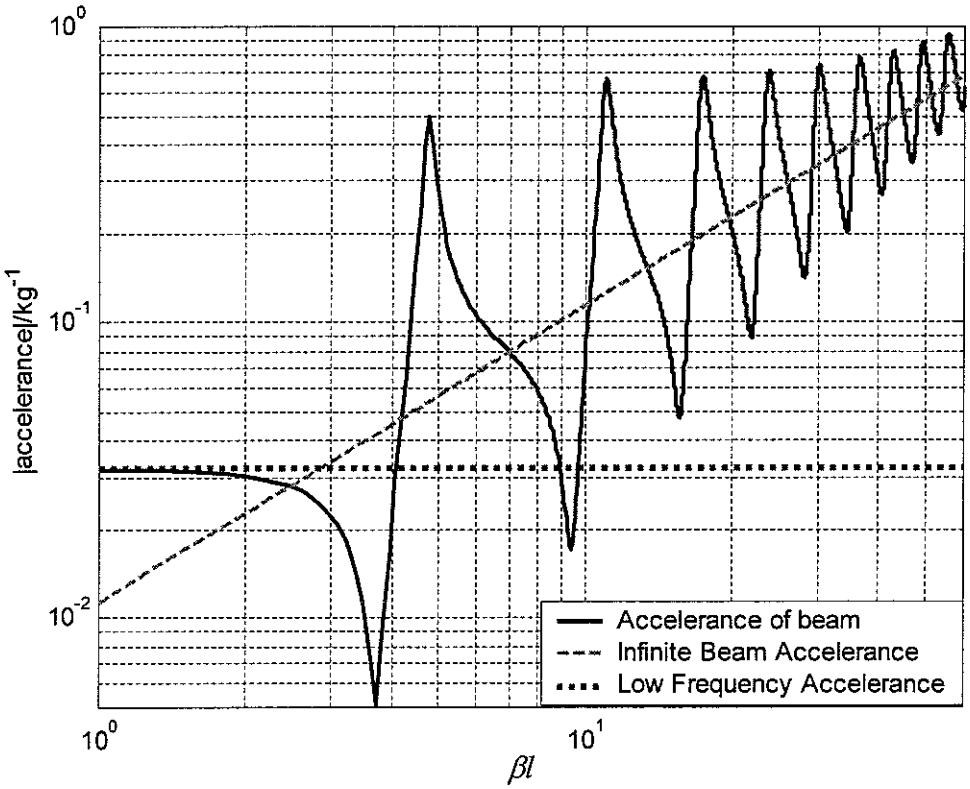

Figure 2.3 Point accelerance for a 2m uniform rectangular cross section steel beam with 10% proportional damping with a point force applied in the centre, to an infinite beam and to a rigid beam.

At low frequencies it can be seen that the beam can be considered to be a rigid mass undergoing translational motion only. At high frequencies, as the number of wavelengths along the beam increases, the behaviour of the beam approaches that of an infinite beam.

2.4 Energy of a forced thin beam with free ends

It is useful to consider the energy of a vibrating structure because each contribution to the energy is a real quantity, not complex and the time dependence of each contribution can be averaged over a cycle. The energy of a thin beam with free ends consists of contributions due to the elastic strain energy of the beam bending and kinetic energy due to the velocity of the beam

$$E = U + T \tag{2.15}$$

where the instantaneous strain energy U is given by (Warburton,1976;Rao,2004)

$$U = \frac{1}{2}\int_{0^-}^{l} EI\left(\frac{\partial^2 w(x,t)}{\partial x^2}\right)^2 dx \tag{2.16}$$

and the instantaneous kinetic energy T is given by (Warburton,1976; Rao,2004)

$$T = \frac{1}{2}\int_{0}^{l} \rho A\left(\frac{\partial w(x,t)}{\partial t}\right)^2 dx \tag{2.17}$$

Using equation (2.13)

$$\frac{\partial^2 w(x,t)}{\partial x^2} = \sum_{n=1}^{\infty} \frac{\phi_n''(x)\phi_n(x_1)}{m(\omega_n^2(1+j\eta)-\omega^2)} f(x_1)e^{j\omega t} \text{ where } \phi_n'' = \frac{d^2\phi(x)}{dx^2}$$

Since the potential energy given by equation (2.16) contains the second partial derivative of $w(x,t)$ with respect to x, U does not contain any contributions from the rigid body modes. Using the result that the time averaged displacement squared, assuming harmonic variation is given by $\left\langle \mathrm{Re}(w(x,t))^2 \right\rangle_t = \frac{1}{2}|w(x)|^2$, the time averaged potential energy is given by

$$\langle U(\omega)\rangle_t = \frac{1}{4}\int_0^l EI\left|\sum_{n=1}^{\infty}\frac{\phi_n''(x)\phi_n(x_1)}{m(\omega_n^2(1+j\eta)-\omega^2)}f(x_1)\right|^2 dx \tag{2.18}$$

To calculate the kinetic energy requires a partial differentiation of $w(x,t)$ with respect to t, which is

$$\frac{\partial w(x,t)}{\partial t} = j\omega\left(\frac{1}{-m\omega^2}+\frac{3}{-m\omega^2}\left(1-\frac{2x}{l}\right)\left(1-\frac{2x_1}{l}\right)+\sum_{n=1}^{\infty}\frac{\phi_n(x)\phi_n(x_1)}{m(\omega_n^2(1+j\eta)-\omega^2)}\right)f(x_1)e^{j\omega t}$$

The time averaged kinetic energy is given by

$$\langle T(\omega)\rangle_t = \frac{1}{4}\int_0^l \rho A\left|j\omega w(x)\right|^2 dx \tag{2.19}$$

which does contain contributions from the two rigid body modes.

2.4.1 Continuous beam model

For a continuous uniform beam, the integrals in equations 2.18 and 2.19 may be evaluated directly to give

$$\langle U(\omega)\rangle_t = \frac{EIl}{4}\sum_{n=1}^{\infty}\left|\frac{\beta_n^4\phi_n^2(x_1)f^2(x_1)}{m^2(\omega_n^2(1+j\eta)-\omega^2)^2}\right| \tag{2.20}$$

and

$$\langle T(\omega)\rangle_t = \frac{\omega^2 f^2(x_1)}{4m}\left(\frac{1}{\omega^4}+\frac{3\left(1-2\frac{x_1}{l}\right)^2}{\omega^4}+\sum_{n=1}^{\infty}\left|\frac{\phi_n^2(x_1)}{(\omega_n^2(1+j\eta)-\omega^2)^2}\right|\right) \tag{2.21}$$

Generally the kinetic energy in the rigid body modes is comprised of kinetic energy due to translation and kinetic energy due to rotation. This is given by the first two terms in equation (2.21). The time averaged kinetic and strain energies for a 2m beam with 10% proportional damping are shown in figure 2.4, together with the time averaged rigid body kinetic energy. As can be seen the kinetic energy and the strain energies are very different at low βl due to the kinetic energy of the translational rigid body mode. Since the beam is excited in the middle, there is no contribution from the rotational rigid body mode. In figure 2.4, the kinetic energy of the translational rigid body mode is very similar to the total kinetic energy of the beam at low frequencies,

showing that nearly all of the energy is in the translational rigid body mode at frequencies well below the first flexural natural frequency.

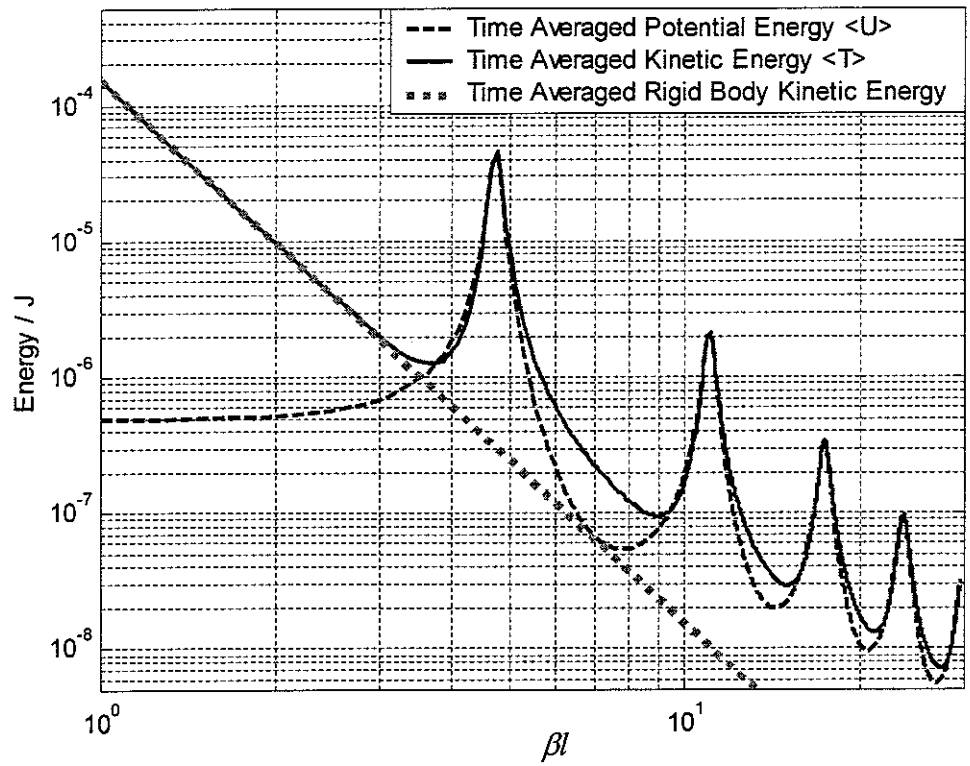

Figure 2.4 Time averaged kinetic and strain energy for a 2m steel beam driven by a single point force in the middle of the beam (x_1=1m). The beam is modelled using 10% proportional damping.

2.4.2 Discretised beam model

Instead of solving equation (2.19) directly, the beam can be considered to consist of P small elements, with mass m_i and width Δx as shown in figure 2.5.

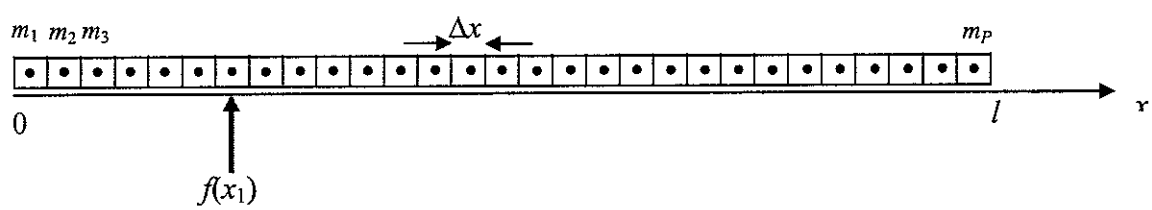

Figure 2.5 Discretised beam consisting of P small elements of width Δx and mass m_i

This model has the advantage that the kinetic energy of the beam can be determined by calculating the lateral displacement at P discrete points along the beam. The displacement is considered in the middle of each element. This mathematical model is

more representative of an experimental determination of the kinetic energy, where typically the lateral displacement can be measured at discrete points along the beam.

Assuming that the elements are small enough to represent the shape of the beam in flexure, for the i^{th} small element of the beam, the kinetic energy is given by

$$T_i = \frac{1}{2}\rho A \Delta x \left(\frac{\partial w(x,t)}{\partial t} \right)^2 \quad \text{where } x = \frac{l}{P}\left(i - \frac{1}{2} \right) \text{ for } i=1 \ldots P$$

So for the whole beam the time averaged kinetic energy is

$$\left\langle T(\omega) \right\rangle_t = \sum_{i=1}^{P} \left. \frac{\rho A l \omega^2 |w(x)|^2}{4P} \right|_{x=i}$$

Substituting for $w(x)$ from equation 2.13 gives

$$\left\langle T(\omega) \right\rangle_t = \sum_{i=1}^{P} \frac{\omega^2 f^2(x_1)}{4Pm} \left(\frac{1+9\left(1-2\frac{x_i}{l}\right)^2\left(1-2\frac{x_1}{l}\right)^2}{\omega^4} + \sum_{n=1}^{\infty} \left| \frac{\phi_n^2(x_i)\phi_n^2(x_1)}{\left(\omega_n^2(1+j\eta)-\omega^2\right)^2} \right| \right) \tag{2.22}$$

where m is the mass of the whole beam and instead of integrating the square of the modeshape along the beam, $\phi_n^2(x)$ is evaluated at discrete points given by $x_i = \frac{l}{P}\left(i - \frac{1}{2} \right)$ for $i=1 \ldots P$

Figure 2.6 shows how this formulation, using $P=51$ elements, compares with the kinetic energy using the continuous beam model, when a point force is applied to the middle of the beam. It can be seen that there is very good agreement between equations (2.21) and (2.22).

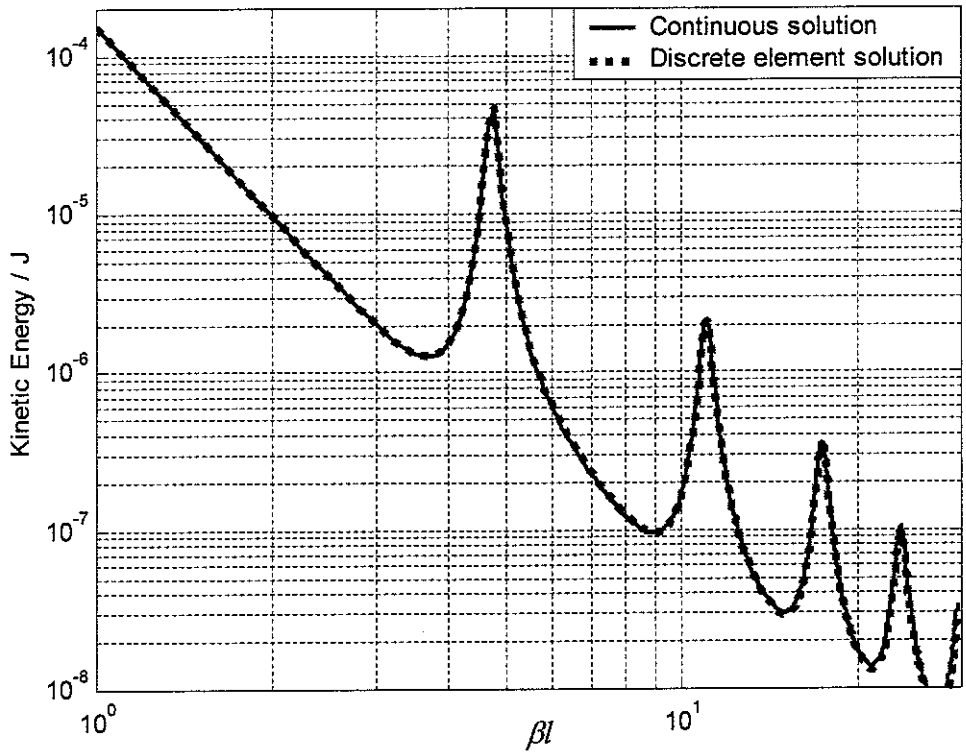

Figure 2.6 Kinetic energy calculated using the continuous beam model (equation 2.21) and the discrete beam model (equation 2.22) with 51 elements. A proportional damping of 10% has been assumed.

Figure 2.7 shows the effect of varying the number of discrete elements by plotting the percentage error in time averaged kinetic energy, relative to the continuous beam solution given by

$$\text{error} = \frac{\text{discrete solution - continuous solution}}{\text{continuous solution}} \times 100\%$$

The number of elements per wavelength at 1 kHz (βl=29.5) is represented by N. As can be seen from figure 2.7, to accurately reproduce the kinetic energy requires greater than 5 elements per wavelength.

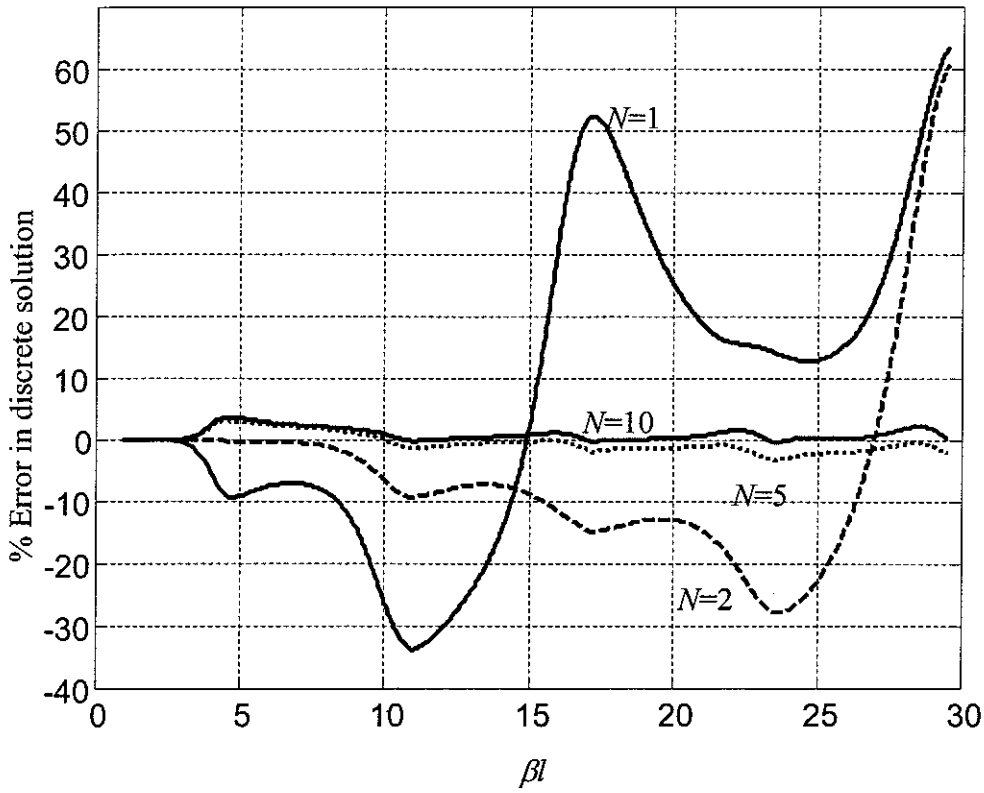

Figure 2.7 The effect of increasing the number of discrete elements P on the kinetic energy discrete beam model. N = the number of elements per wavelength at 1 kHz (βl=29.5).

2.5 Hermitian quadratic form for the kinetic energy of a thin beam with free ends driven by two point forces

In the previous section, models were developed for the time averaged kinetic energy of a beam with free ends when a single point force is applied. In this section the kinetic energy of the beam under the action of two point forces is considered. For the continuous beam model and the discrete beam model, the total time averaged kinetic energy can be written in a concise vector notation using the Hermitian quadratic form. Section 2.6 explains why this Hermitian form is useful and how the second force can be applied in such a way that the overall time averaged kinetic energy when two forces are applied is lower than that when a single force is applied.

Although only two point forces are considered in this report, the vector notation may be generalised to describe the kinetic energy of the beam when it is driven by many

forces.

Figure 2.8 shows the beam with two point forces applied at $x=x_1$ and $x=x_2$.

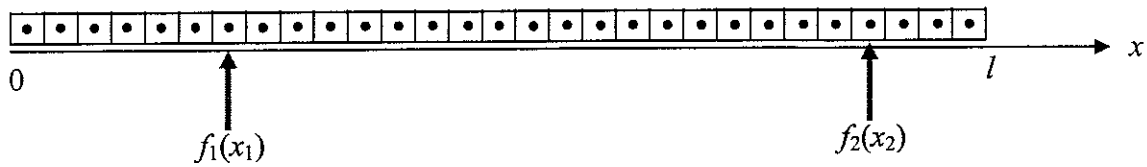

Figure 2.8 Beam with free end conditions and two applied point forces

Using equation 2.12, the principle of superposition and assuming that the two applied point forces excite the beam at the same frequency, then

$$w(x,t)=\sum_{n=0}^{\infty}\phi_n(x)\left[q_{1,n}(t)+q_{2,n}(t)\right]=\sum_{n=0}^{\infty}\frac{\phi_n(x)\left[\phi_n(x_1)f_1(x_1)+\phi_n(x_2)f_2(x_2)\right]}{m(\omega_n^2(1+j\eta)-\omega^2)}\,e^{j\omega t} \qquad (2.23)$$

Where f_1 and f_2 can be complex to allow for phase differences between the point forces, and $q_{1,n}$ is the n^{th} modal amplitude due to the primary force f_1 at x_1 and $q_{2,n}$ is the n^{th} modal amplitude due to the secondary force f_2 at x_2.

2.5.1 Continuous beam model

Using equation (2.21) and following a similar procedure to that described in section 2.4.1 for a single applied force, the time averaged kinetic energy of a free-free beam with two applied forces can be written as

$$\left\langle T(\omega)\right\rangle_t=\frac{\omega^2}{4m}\sum_{n=0}^{\infty}\left|\frac{\left[f_1(x_1)\phi_n(x_1)+f_2(x_2)\phi_n(x_2)\right]}{(\omega_n^2(1+j\eta)-\omega^2)}\right|^2 \qquad (2.24)$$

where the n^{th} modal amplitude due to each force is given by

$$q_{1,n}(\omega)=\frac{\phi_n(x_1)f_1(x_1)}{m(\omega_n^2(1+j\eta)-\omega^2)} \quad \text{and} \quad q_{2,n}(\omega)=\frac{\phi_n(x_2)f_2(x_2)}{m(\omega_n^2(1+j\eta)-\omega^2)}$$

This enables the time averaged kinetic energy to be written as

$$\left\langle T(\omega)\right\rangle_t=\frac{m\omega^2}{4}\sum_{n=0}^{\infty}\left|q_{1,n}+q_{2,n}\right|^2$$

Defining $\mathbf{q}$ as a vector of modal amplitudes over n modes such that

$$\mathbf{q} = \begin{bmatrix} q_{1,1} + q_{2,1} \\ q_{1,2} + q_{2,2} \\ q_{1,3} + q_{2,3} \\ \vdots \\ q_{1,n} + q_{2,n} \end{bmatrix}$$

The time averaged kinetic energy of the beam can be written as

$$\langle T(\omega) \rangle_t = \frac{m\omega^2}{4} \mathbf{q}^H(\omega)\mathbf{q}(\omega) \tag{2.25}$$

Where the Hermitian form $\mathbf{q}^H$ is the complex conjugate transpose of vector $\mathbf{q}$. This concise notation can be extended to incorporate any number of point forces in the vector $\mathbf{q}$.

2.5.2 Discretised beam model

Extending the results from section 2.4.2 to two applied forces

$$\langle T(\omega) \rangle_t = \sum_{i=1}^{P} \frac{\rho A l \omega^2 |w(x)|^2}{4P} = \sum_{i=1}^{P} \frac{\rho A l \omega^2}{4P} \sum_{n=0}^{\infty} \left| \frac{\phi_n(x)[\phi_n(x_1) f_1(x_1) + \phi_n(x_2) f_2(x_2)]}{m(\omega_n^2(1+j\eta) - \omega^2)} \right|^2$$

Defining $\mathbf{w}$ as a vector of displacements over n modes including the two rigid body modes

$$\mathbf{w} = \begin{bmatrix} \dfrac{\phi_1(x)\ [\phi_1(x_1) f_1(x_1) + \phi_1(x_2) f_2(x_2)]}{m(\omega_1^2(1+j\eta) - \omega^2)} \\ \dfrac{\phi_2(x)\ [\phi_2(x_1) f_1(x_1) + \phi_2(x_2) f_2(x_2)]}{m(\omega_2^2(1+j\eta) - \omega^2)} \\ \dfrac{\phi_3(x)\ [\phi_3(x_1) f_1(x_1) + \phi_3(x_2) f_2(x_2)]}{m(\omega_3^2(1+j\eta) - \omega^2)} \\ \vdots \\ \dfrac{\phi_n(x)\ [\phi_n(x_1) f_1(x_1) + \phi_n(x_2) f_2(x_2)]}{m(\omega_n^2(1+j\eta) - \omega^2)} \end{bmatrix}$$

The time averaged kinetic energy of the discrete beam can be written in vector form as

$$\langle T(\omega)\rangle_t = \sum_{i=1}^{P} \frac{m\omega^2}{4P} \mathbf{w}_i{}^H \mathbf{w}_i \qquad (2.26)$$

2.6 Using the Hermitian form to minimise the Kinetic Energy

The total time averaged kinetic energy of a beam with free ends, when two or more point forces are applied to the beam, is given by equations 2.25 and 2.26 for the continuous and discrete models respectively. The reason for expressing the kinetic energy in the compact Hermitian quadratic form is that methods exist to minimise the total kinetic energy of the beam by altering the position, magnitude and phase of any secondary forces that may be applied for control (Nelson and Elliott, 1992, Appendix). The optimum magnitude and phase of the secondary forces can be determined, so that the time averaged kinetic energy of the beam driven by primary and secondary point forces is lower than the time averaged kinetic energy of the beam with only a primary force applied.

2.6.1 Continuous beam model

The vector of modal amplitudes from section 2.5.1 can be written in terms of the superposition of the modal amplitudes due to the primary force alone and the modal amplitudes due to an array of secondary forces, so that $\mathbf{q} = \mathbf{q}_1 + \mathbf{B}\,\mathbf{f}_s$. $\mathbf{B}$ is a matrix of modal coupling coefficients. Equation 2.25 can be written in the standard Hermitian quadratic form as

$\langle T(\omega)\rangle_t = \frac{m\omega^2}{4}\mathbf{q}^H(\omega)\mathbf{q}(\omega)$ substituting for $\mathbf{q} = \mathbf{q}_1 + \mathbf{B}\,\mathbf{f}_s$ and expanding gives

$$\langle T(\omega)\rangle_t = \frac{m\omega^2}{4}\left(\mathbf{q}_1{}^H\mathbf{q}_1 + \mathbf{q}_1{}^H\mathbf{B}\mathbf{f}_s + \mathbf{f}_s{}^H\mathbf{B}^H\mathbf{q}_1 + \mathbf{f}_s{}^H\mathbf{B}^H\mathbf{B}\mathbf{f}_s\right)$$

which corresponds to the standard Hermitian quadratic form described by Nelson and Elliott as

$$J = c + \mathbf{b}^H\mathbf{x} + \mathbf{x}^H\mathbf{b} + \mathbf{x}^H\mathbf{A}\mathbf{x}$$

$$\text{with } c = \mathbf{q}_1{}^H\mathbf{q}_1,\ \mathbf{b} = \mathbf{B}^H\mathbf{q}_1,\ \ \mathbf{A} = \mathbf{B}^H\mathbf{B},\ \ \mathbf{x} = \mathbf{f}_s$$

This has a minimum when $\mathbf{x}_0 = -\mathbf{A}^{-1}\mathbf{b}$, which for the general case of many secondary forces gives a minimum time averaged kinetic energy when $\mathbf{f}_s = -\left[\mathbf{B}^H\mathbf{B}\right]^{-1}\mathbf{B}^H\mathbf{q}_1$.

Considering the case of a single secondary force f_2, the vector of modal amplitudes can be written as

$$\mathbf{q} = \mathbf{q}_1 + \mathbf{q}_2 = \begin{bmatrix} q_{1,1} \\ \vdots \\ q_{1,n} \end{bmatrix} + \begin{bmatrix} q_{2,1} \\ \vdots \\ q_{2,n} \end{bmatrix}$$

Using $q_{2,n}(\omega) = \dfrac{\phi_n(x_2) f_2(x_2)}{m(\omega_n^2(1+j\eta)-\omega^2)}$

$$\mathbf{q} = \begin{bmatrix} q_{1,1} \\ \vdots \\ q_{1,n} \end{bmatrix} + \begin{bmatrix} \dfrac{\phi_1(x_2)}{m(\omega_1^2(1+j\eta)-\omega^2)} \\ \vdots \\ \dfrac{\phi_n(x_2)}{m(\omega_n^2(1+j\eta)-\omega^2)} \end{bmatrix} f_2$$

The minimum kinetic energy occurs when

$$f_2 = -\left[\mathbf{b}^{\mathrm{H}}\mathbf{b}\right]^{-1}\mathbf{b}^{\mathrm{H}}\mathbf{q}_1 \tag{2.27}$$

where $\mathbf{b}$ is the vector of modal amplitudes generated by f_2.

2.6.2 Discretised beam model

The time averaged kinetic energy for the discretised beam model was derived in section 2.5.2 and is repeated here for convenience.

$$\langle T(\omega)\rangle_t = \sum_{i=1}^{P} \frac{m\omega^2}{4P} \mathbf{w}_i^{\,H} \mathbf{w}_i \tag{2.26}$$

For the general case of r secondary forces, the displacement can be written as

$$w(x,\omega) = \sum_{n=0}^{\infty} \left[\frac{\phi_n(x)\phi_n(x_1) f_1}{m(\omega_n^2(1+j\eta)-\omega^2)} + \sum_{i=2}^{r+1} \frac{\phi_n(x)\phi_n(x_i) f_i}{m(\omega_n^2(1+j\eta)-\omega^2)} \right]$$

using the notation for modal amplitudes from section 2.6.1 this can be written

$w(x,\omega) = \boldsymbol{\varphi}^T \mathbf{q}_1 + \boldsymbol{\varphi}^T \left[\mathbf{q}_2 + \mathbf{q}_3 + \cdots \mathbf{q}_{r+1}\right]$ where $\boldsymbol{\varphi}^T = \left[\phi_0(x) \quad \cdots \quad \phi_n(x)\right]$ over n modes.

Defining $\boldsymbol{\beta}$ as an n x r matrix of the form

$$\begin{bmatrix} \dfrac{\phi_0(x_2)}{m(\omega_1^2(1+j\eta)-\omega^2)} & \cdots & \dfrac{\phi_0(x_{r+1})}{m(\omega_1^2(1+j\eta)-\omega^2)} \\ \vdots & \cdots & \vdots \\ \dfrac{\phi_n(x_2)}{m(\omega_n^2(1+j\eta)-\omega^2)} & \cdots & \dfrac{\phi_n(x_{r+1})}{m(\omega_n^2(1+j\eta)-\omega^2)} \end{bmatrix}$$

and $\boldsymbol{\alpha}$ as a vector of the form $\begin{bmatrix} \dfrac{\phi_0(x_1)}{m(\omega_1^2(1+j\eta)-\omega^2)} \\ \vdots \\ \dfrac{\phi_n(x_1)}{m(\omega_1^2(1+j\eta)-\omega^2)} \end{bmatrix}$

the beam displacement can be written as $w(x,\omega) = \boldsymbol{\varphi}^T\boldsymbol{\alpha}f_1 + \boldsymbol{\varphi}^T\boldsymbol{\beta}\mathbf{f}_s$ where $\mathbf{f}_s = \begin{bmatrix} f_2 \\ \vdots \\ f_{r+1} \end{bmatrix}$

Each discrete element has a time averaged kinetic energy

$$\langle T_i(\omega)\rangle_t = \frac{m\omega^2}{4P}\left[\boldsymbol{\varphi}_i^T\boldsymbol{\alpha}f_1 + \boldsymbol{\varphi}_i^T\boldsymbol{\beta}\mathbf{f}_s\right]^H\left[\boldsymbol{\varphi}_i^T\boldsymbol{\alpha}f_1 + \boldsymbol{\varphi}_i^T\boldsymbol{\beta}\mathbf{f}_s\right]$$

hence the total time averaged kinetic energy is given by

$$\langle T(\omega)\rangle_t = \sum_{i=1}^{P}\frac{m\omega^2}{4P}\left[\boldsymbol{\varphi}_i^T\boldsymbol{\alpha}f_1 + \boldsymbol{\varphi}_i^T\boldsymbol{\beta}\mathbf{f}_s\right]^H\left[\boldsymbol{\varphi}_i^T\boldsymbol{\alpha}f_1 + \boldsymbol{\varphi}_i^T\boldsymbol{\beta}\mathbf{f}_s\right] \tag{2.28}$$

which can be expanded to give

$$\langle T(\omega)\rangle_t = \sum_{i=1}^{P}\frac{m\omega^2}{4P}\left[f_1^*\boldsymbol{\alpha}^H\boldsymbol{\varphi}_i^*\boldsymbol{\varphi}_i^T\boldsymbol{\alpha}f_1 + f_1^*\boldsymbol{\alpha}^H\boldsymbol{\varphi}_i^*\boldsymbol{\varphi}_i^T\boldsymbol{\beta}\mathbf{f}_s + \mathbf{f}_s{}^H\boldsymbol{\beta}^H\boldsymbol{\varphi}_i^*\boldsymbol{\varphi}_i^T\boldsymbol{\alpha}f_1 + \mathbf{f}_s{}^H\boldsymbol{\beta}^H\boldsymbol{\varphi}_i^*\boldsymbol{\varphi}_i^T\boldsymbol{\beta}\mathbf{f}_s\right]$$

This can be compared to the notation of Nelson and Elliott

$$J = c + \mathbf{b}^H\mathbf{x} + \mathbf{x}^H\mathbf{b} + \mathbf{x}^H\mathbf{A}\mathbf{x}$$

where $c = \sum_{i=1}^{P}\boldsymbol{\alpha}^H\boldsymbol{\varphi}_i^*\boldsymbol{\varphi}_i^T\boldsymbol{\alpha}|f_1|^2$, $\mathbf{b} = \sum_{i=1}^{P}\boldsymbol{\beta}^H\boldsymbol{\varphi}_i^*\boldsymbol{\varphi}_i^T\boldsymbol{\alpha}f_1$, $\mathbf{A} = \sum_{i=1}^{P}\boldsymbol{\beta}^H\boldsymbol{\varphi}_i^*\boldsymbol{\varphi}_i^T\boldsymbol{\beta}$, $\mathbf{x} = \mathbf{f}_s$

This has a minimum when $\mathbf{x}_0 = -\mathbf{A}^{-1}\mathbf{b}$, which gives a minimum kinetic energy for the general case of r secondary forces when $\mathbf{f}_s = -\left[\sum_{i=1}^{P}\boldsymbol{\beta}^H\boldsymbol{\varphi}_i^*\boldsymbol{\varphi}_i^T\boldsymbol{\beta}\right]^{-1}\sum_{i=1}^{P}\boldsymbol{\beta}^H\boldsymbol{\varphi}_i^*\boldsymbol{\varphi}_i^T\boldsymbol{\alpha}f_1$

Considering the case of the discrete beam model with a single secondary force

$$\langle T(\omega)\rangle_t = \sum_{i=1}^{P} \frac{m\omega^2 |f_1|^2}{4P} \left[\boldsymbol{\alpha}^H \boldsymbol{\varphi}_i^* \boldsymbol{\varphi}_i^T \boldsymbol{\alpha} + \boldsymbol{\alpha}^H \boldsymbol{\varphi}_i^* \boldsymbol{\varphi}_i^T \boldsymbol{\beta} \frac{f_2}{f_1} + \left(\frac{f_2}{f_1}\right)^* \boldsymbol{\beta}^H \boldsymbol{\varphi}_i^* \boldsymbol{\varphi}_i^T \boldsymbol{\alpha} + \left(\frac{f_2}{f_1}\right)^* \boldsymbol{\beta}^H \boldsymbol{\varphi}_i^* \boldsymbol{\varphi}_i^T \boldsymbol{\beta} \frac{f_2}{f_1} \right]$$

which has a minimum kinetic energy when $\frac{f_2}{f_1} = -\left[\sum_{i=1}^{P} \boldsymbol{\beta}^H \boldsymbol{\varphi}_i^* \boldsymbol{\varphi}_i^T \boldsymbol{\beta}\right]^{-1} \sum_{i=1}^{P} \boldsymbol{\beta}^H \boldsymbol{\varphi}_i^* \boldsymbol{\varphi}_i^T \boldsymbol{\alpha}$

2.6.3 Rigid Body Model

The kinetic energy in the rigid body modes for two applied forces is given by

$$\langle T_{rb}(\omega)\rangle_t = \frac{1}{4m\omega^2} \left[(f_1 + f_2)^2 + 3\left(f_1\left(1 - 2\frac{x_1}{l}\right) + f_2\left(1 - 2\frac{x_2}{l}\right)\right)^2 \right] \tag{2.29}$$

This can be expressed in vector form as

$$\langle T_{rb}(\omega)\rangle_t = \frac{1}{4m\omega^2} \mathbf{q}^H \mathbf{q}$$

where $\mathbf{q}$ is the vector such that

$$\mathbf{q} = \left[\sqrt{3}\left(1 - 2\frac{x_1}{l}\right)\right] f_1 + \left[\sqrt{3}\left(1 - 2\frac{x_2}{l}\right)\right] f_2$$

which is of the form $\mathbf{q} = \mathbf{q}_1 + \mathbf{b} f_2$ where $\mathbf{b} = \left[\sqrt{3}\left(1 - 2\frac{x_2}{l}\right)\right]$

Using the same method as section 2.6.1

$$\mathbf{q}^H \mathbf{q} = \mathbf{q}_1^H \mathbf{q}_1 + \mathbf{q}_1^H \mathbf{b} f_2 + f_2^* \mathbf{b}^H \mathbf{q}_1 + f_2^* \mathbf{b}^H \mathbf{b} f_2$$

This has a minimum kinetic energy when $f_2 = -\left[\mathbf{b}^H \mathbf{b}\right]^{-1} \mathbf{b}^H \mathbf{q}_1$, i.e. when

$$f_2 = -f_1 \frac{\left[1 + 3\left(1 - 2\frac{x_1}{l}\right)\left(1 - 2\frac{x_2}{l}\right)\right]}{\left[1 + 3\left(1 - 2\frac{x_2}{l}\right)^2\right]} \tag{2.30}$$

The minimum time averaged kinetic energy can be found by substituting equation (2.30) into equation (2.29)

$$\frac{\langle T_{\min}(\omega)\rangle_t}{|f_1|^2}=\frac{1}{4m\omega^2}\left[\left(1-\frac{1+3\left(1-2\frac{x_1}{l}\right)\left(1-2\frac{x_2}{l}\right)}{1+3\left(1-2\frac{x_2}{l}\right)^2}\right)^2+3\left(\left(1-2\frac{x_1}{l}\right)-\left(1-2\frac{x_2}{l}\right)\frac{1+3\left(1-2\frac{x_1}{l}\right)\left(1-2\frac{x_2}{l}\right)}{1+3\left(1-2\frac{x_2}{l}\right)^2}\right)^2\right]$$

(2.31)

3 Numerical simulations of the minimisation of the total time averaged kinetic energy in a beam

Figure 3.1 shows an example of using a secondary force near the centre of the beam to reduce the overall time averaged kinetic energy of the beam driven by a central primary force.

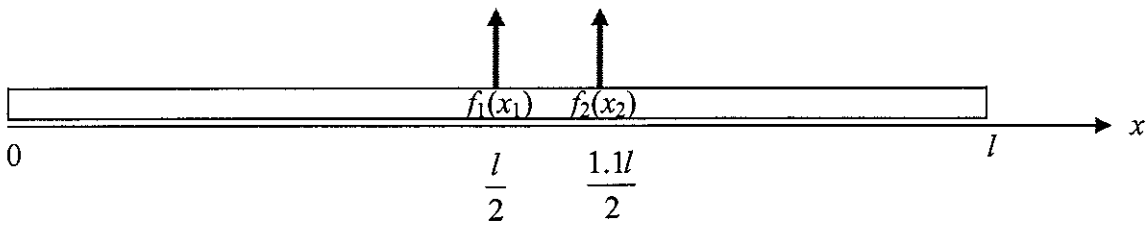

Figure 3.1 Controlling the time averaged kinetic energy of a beam driven by a central primary force with a secondary force near the centre.

The optimum value for f_2 in order to minimise the time-averaged kinetic energy of the beam at each frequency has been determined using equation 2.27. This has then been used in equation 2.25 to calculate the total time averaged kinetic energy of the beam driven by the two forces. This is presented in figure 3.2.

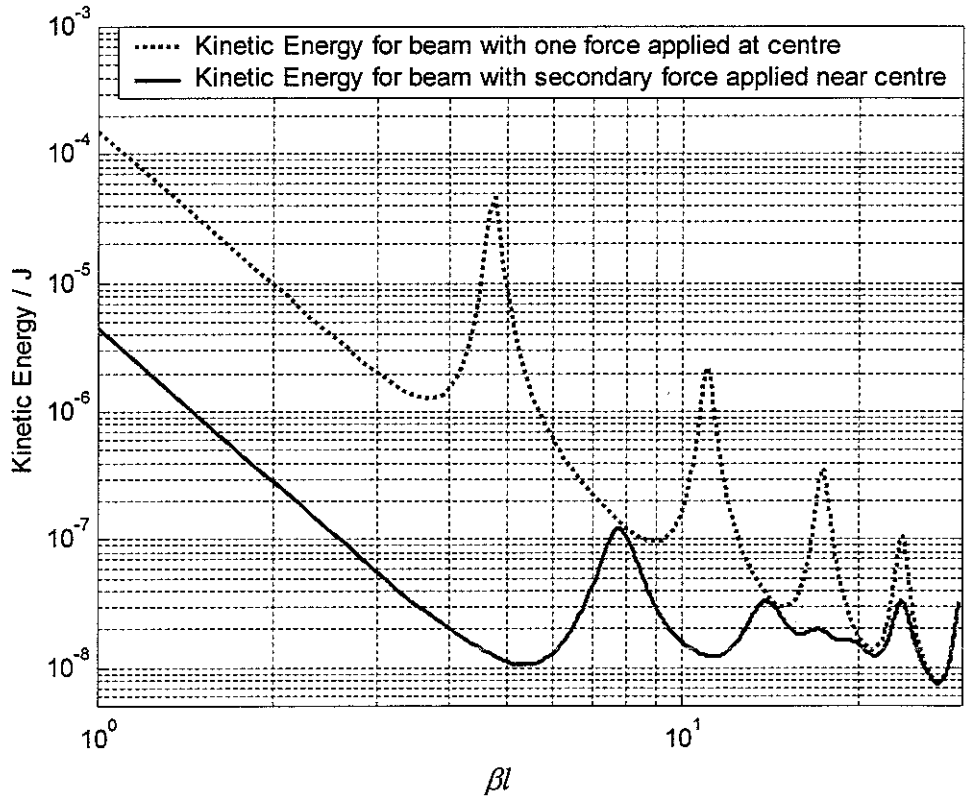

Figure 3.2 Total time averaged kinetic energy for a beam driven by a single force applied at the centre, and for a beam with an additional secondary force near the centre. The magnitude and phase of the secondary force have been chosen to minimise the overall kinetic energy at each frequency.

Figures 3.3 and 3.4 show the results for a secondary force applied near the end of the beam in order to reduce the overall time averaged kinetic energy of the beam with the primary force still applied at the centre.

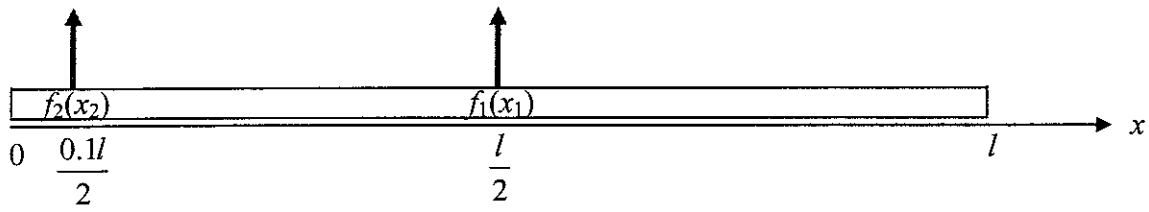

Figure 3.3 Controlling the time averaged kinetic energy of a beam driven by a central primary force with a secondary force near the end.

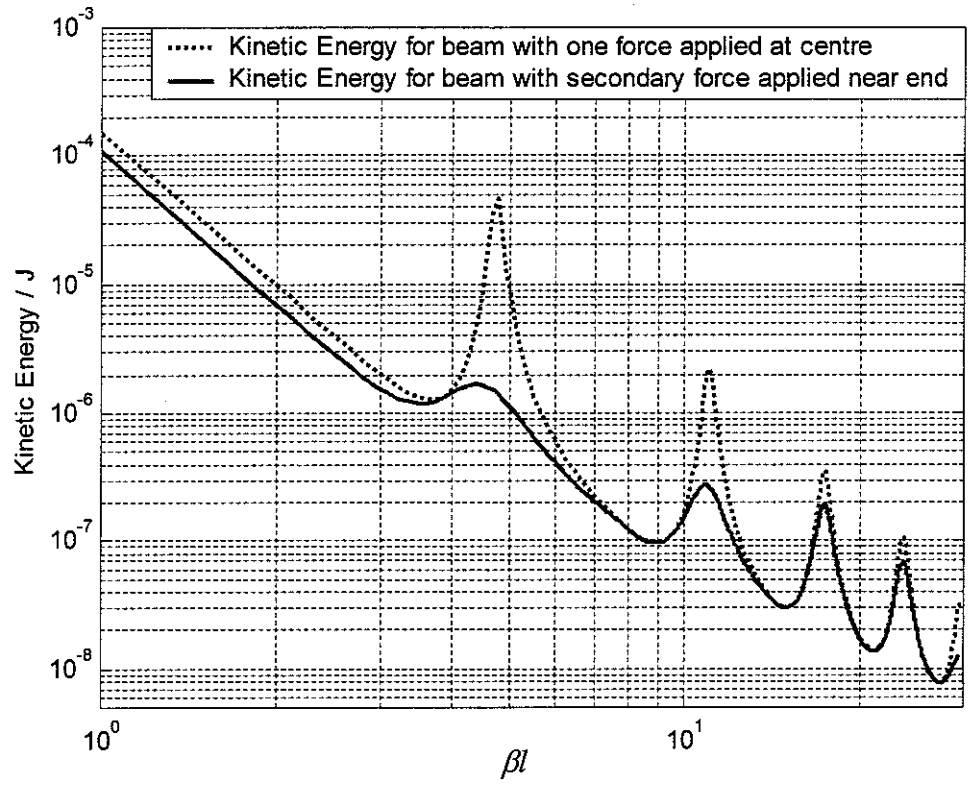

Figure 3.4 Total time averaged kinetic energy for a beam driven by a single force applied at the centre, and for a beam with an additional secondary force near the end. The magnitude and phase of the secondary force have been chosen to minimise the overall kinetic energy at each frequency.

Figure 3.2 shows that the application of the secondary force near to the primary force has reduced the overall time averaged kinetic energy of the beam. Figure 3.4 shows that the application of a secondary force near one end of the beam is also able to reduce the kinetic energy of the beam, but not to the same extent as shown in figure 3.2.

Figure 3.5 shows the cumulative kinetic energy for a beam, driven by a single point force at one end, summed up to 5 kHz (βl=66), which includes the first 20 non-rigid modes. The cumulative energy is shown as a percentage of the total sum up to 5 kHz.

$$\text{cumulative \% total kinetic energy}(f) = \frac{\sum_{i=1}^{f} \langle T(i) \rangle_t}{\sum_{i=1}^{5000} \langle T(i) \rangle_t} \times 100$$

A beam driven at one end is considered so that all of the modes are excited.

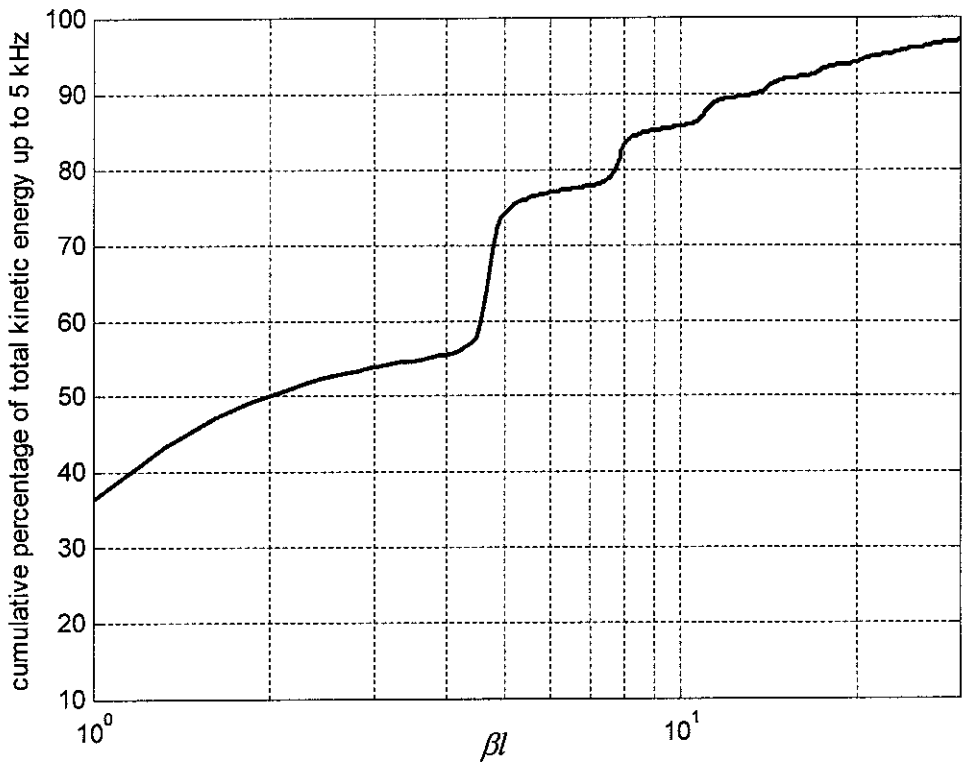

Figure 3.5 Cumulative kinetic energy for a free-free beam driven at one end by a point force. Shown as a percentage of the total sum up to 5 kHz (βl=66) which includes the first 20 flexible modes.

Figure 3.5 shows that between 40% and 50% of the total energy up to 5 kHz is in the two rigid body modes. This suggests that a simple optimisation scheme to reduce the kinetic energy in the rigid body modes would significantly reduce the overall kinetic energy of the beam. Equation (2.30) can be used to produce a minimisation of the kinetic energy in the rigid body modes. In this case the secondary force f_2 as given by equation (2.30) is constant for all frequencies and reduces to $f_2 = -f_1$ if the secondary force is coincident with the primary force.

Figure 3.6 shows the kinetic energy in the rigid body modes for the situation described by figure 3.1, for a single central point force and for a secondary force near the centre optimised to reduce the kinetic energy in the rigid body modes by using equation (2.30). Also shown in figure 3.6 is the total kinetic energy using equation (2.21) for a beam driven by a single central force and the kinetic energy obtained

from equation (2.24) for the beam driven by two point forces. In this case the magnitude and phase of f_2 have not been optimised at each frequency, instead the value determined to minimise the kinetic energy of the rigid body modes using equation (2.30) has been applied at all frequencies. This is in contrast to figure 3.2 where the minimisation was determined at each frequency.

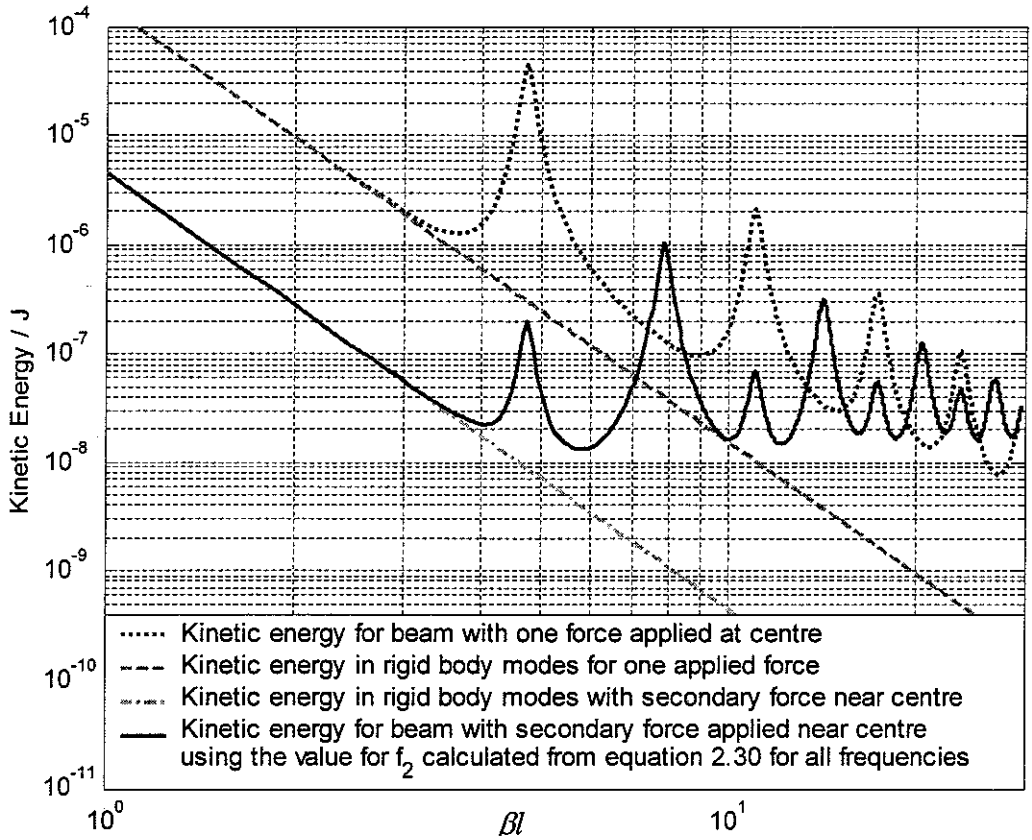

Figure 3.6 Total time averaged kinetic energy using a) single force equation (2.21) with 50 flexible modes b) rigid body equation (2.29) for (i) a beam driven by a single force applied at the centre (ii) for a beam with an additional secondary force near the centre and c) two force equation (2.24) with 50 flexible modes and the magnitude and phase of the secondary force chosen to minimise the rigid body kinetic energy as given in equation (2.30) then applied to each frequency.

Figure 3.6 clearly shows that the secondary force when optimised can reduce the energy in the rigid body modes for this orientation of the forces. The solid curve shows that using the same magnitude and phase for the secondary force for all frequencies introduces energy into the even numbered modes that were not excited by the single central force. Using a full optimisation of f_2 at each frequency, as described by equation (2.27) and shown in figure 3.2, gives lower values for time averaged kinetic energy than an optimisation using just the rigid body modes.

Figure 3.7 shows the magnitude of f_2/f_1 obtained from equation (2.27), together with the phase of f_2 with respect to f_1 for the case depicted in figure 3.1. As can be seen from figure 3.7, the amplitude of f_2 is small at frequencies corresponding to the even modes of the beam such as βl=7.8. These even modes are not excited when f_2 is not present. These low amplitudes ensure that the optimised control force f_2 does not increase the overall kinetic energy at these frequencies by effectively 'switching it off'. This is also clear in figure 3.2 at βl=7.8.

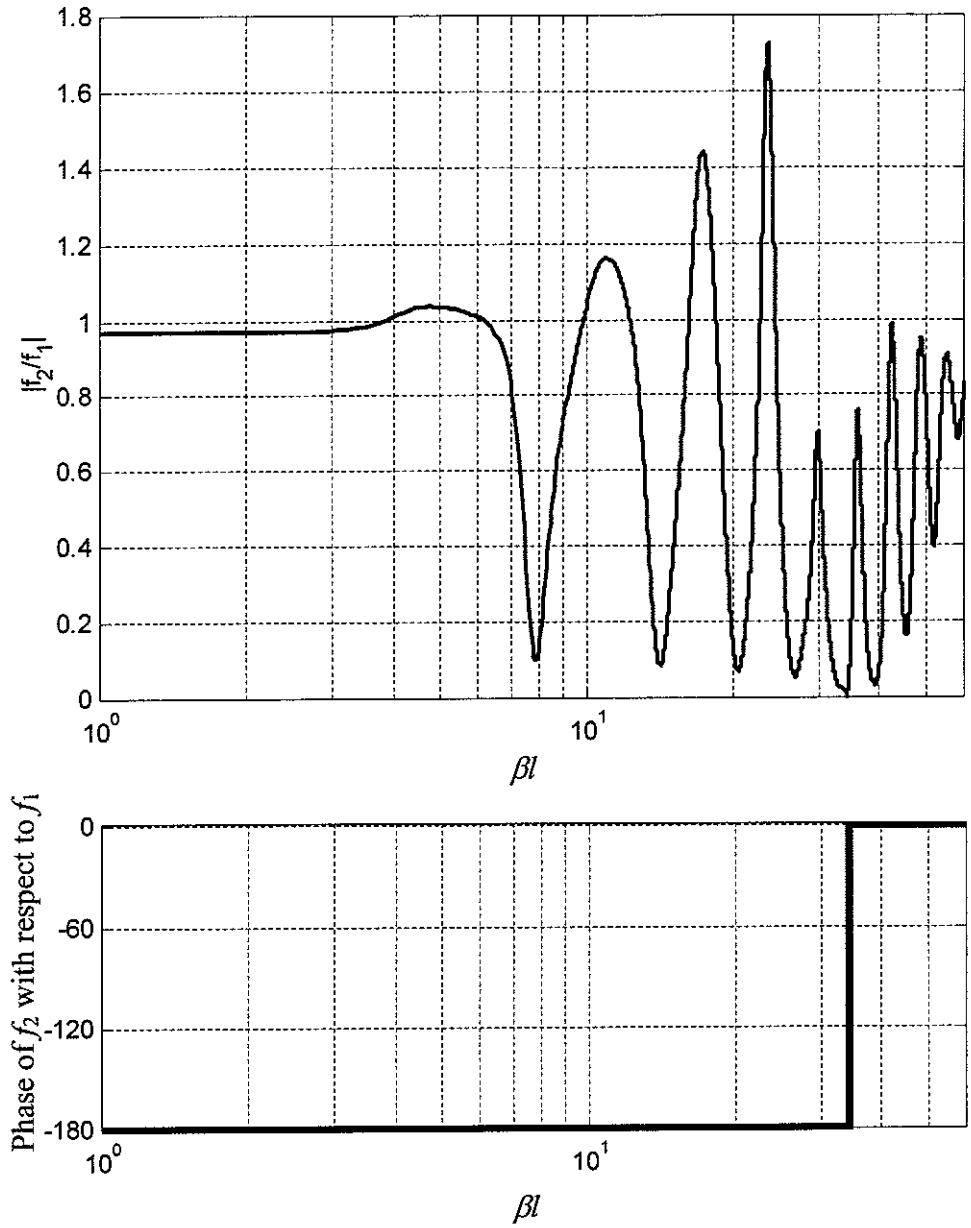

Figure 3.7 Amplitude and phase of f_2 with respect to f1 for optimisation using equation (2.27) for beam driven by a central primary force and a secondary force near to the centre as shown in figure 3.1

The cumulative kinetic energy - for the force positions shown in figure 3.1 - as a percentage of the total kinetic energy of the beam driven by a single central point force up to 5 kHz is presented in figure 3.8. The total amount of kinetic energy in frequencies below 5 kHz - which corresponds to the first 20 flexural modes of the beam - is much lower if the simple rigid body minimisation is performed, and even lower if the full minimisation at each frequency is performed.

Figure 3.4 showed that, for some positions of the secondary force, the overall kinetic energy of the beam does not get reduced to a great extent. For the situation shown in figure 3.3 - with the secondary force close to one end - the simple rigid body minimisation of equation (2.30) applied at all frequencies causes the beam to have more kinetic energy than when just the single central force is applied for frequencies below 5 kHz, as shown in figure 3.9. For this configuration of primary and secondary force, it would be unwise to apply the rigid body minimisation value of f_2 at all frequencies.

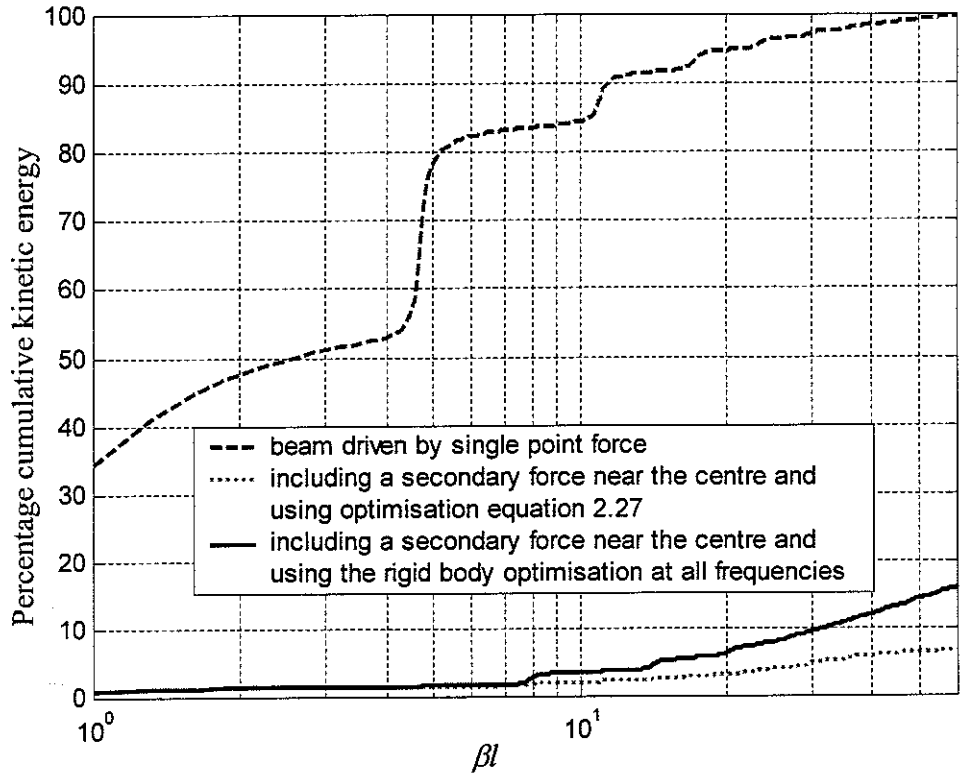

Figure 3.8 The cumulative time averaged kinetic energy as a percentage of the kinetic energy when the beam is driven by a single central point force (at x/l=0.5). a) for the beam driven by a single point force, b) for the beam with a secondary force near to the centre (at x/l=0.55) and using the full minimisation at each frequency, c) for the beam with a secondary force near to the centre (at x/l=0.55)

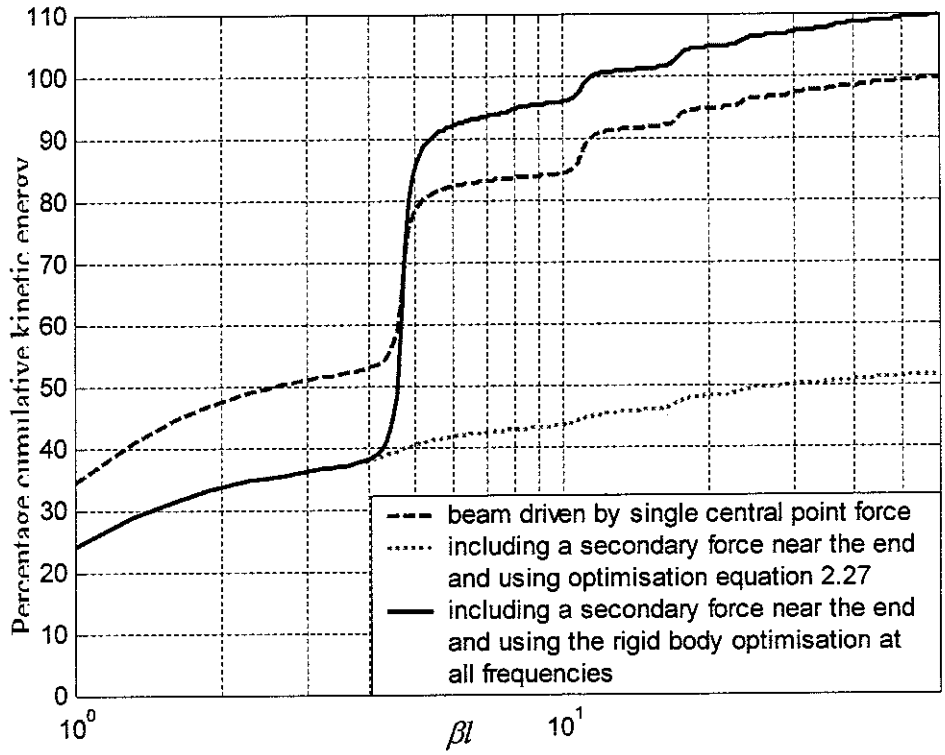

Figure 3.9 The cumulative time averaged kinetic energy as a percentage of the kinetic energy when the beam is driven by a single central point force (at x/l=0.5). a) for the beam driven by a single point force, b) for the beam with a secondary force near to the end (at x/l=0.05) and using the full minimisation at each frequency, c) for the beam with a secondary force near to the end (at x/l=0.05) and using the rigid body minimisation at all

4 Discussion

The rigid body model can be used to predict how useful a secondary force in a particular position will be in reducing the overall kinetic energy of the beam. Using equation (2.30)

$$f_2 = -f_1 \frac{\left[1+3\left(1-2\frac{x_1}{l}\right)\left(1-2\frac{x_2}{l}\right)\right]}{\left[1+3\left(1-2\frac{x_2}{l}\right)^2\right]} \tag{2.30}$$

the overall time averaged kinetic energy of the beam will not be reduced when f_2=0.0 i.e. when

$$3\left(1-2\frac{x_1}{l}\right)\left(1-2\frac{x_2}{l}\right) = -1$$

$$\frac{x_2}{l} = \frac{1}{2}\left[\frac{1+3\left(1-2\frac{x_1}{l}\right)}{3\left(1-2\frac{x_1}{l}\right)}\right] \tag{4.1}$$

Equation (4.1) gives the position of the secondary force where the overall kinetic energy of the beam is not reduced. This is plotted in figure 4.1.

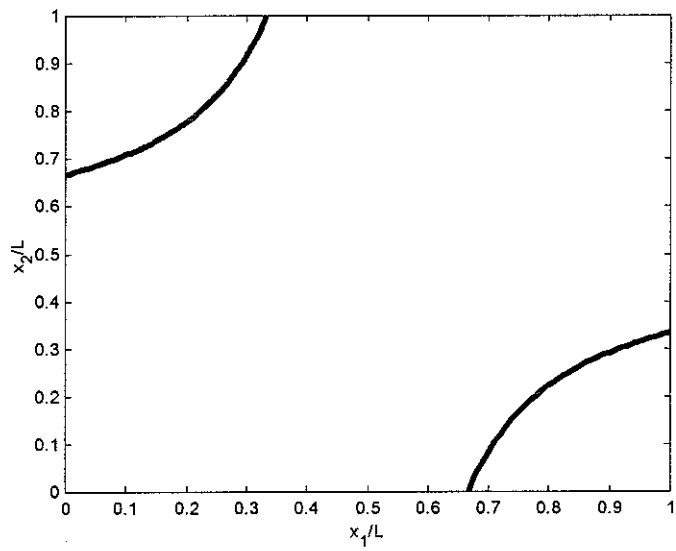

Figure 4.1 Plot of equation 4.1. The position of the secondary force where the overall kinetic energy of the beam is not reduced .

As can be seen from figure 4.1, using the rigid body model, for a primary force on the

interval $\frac{l}{3} < x_1 < \frac{2l}{3}$, the application of a secondary force anywhere on the beam will reduce the overall kinetic energy in the rigid body modes provided the amplitude is chosen according to equation (2.30).

For the primary force x_1 on the intervals $\left[0, \frac{l}{3}\right]$ and $\left[\frac{2l}{3}, l\right]$ there is a position for the secondary force where the kinetic energy cannot be reduced, this position corresponds to the point about which the rigid beam is rotating when the single primary force is applied. Figure 4.2 shows some examples.

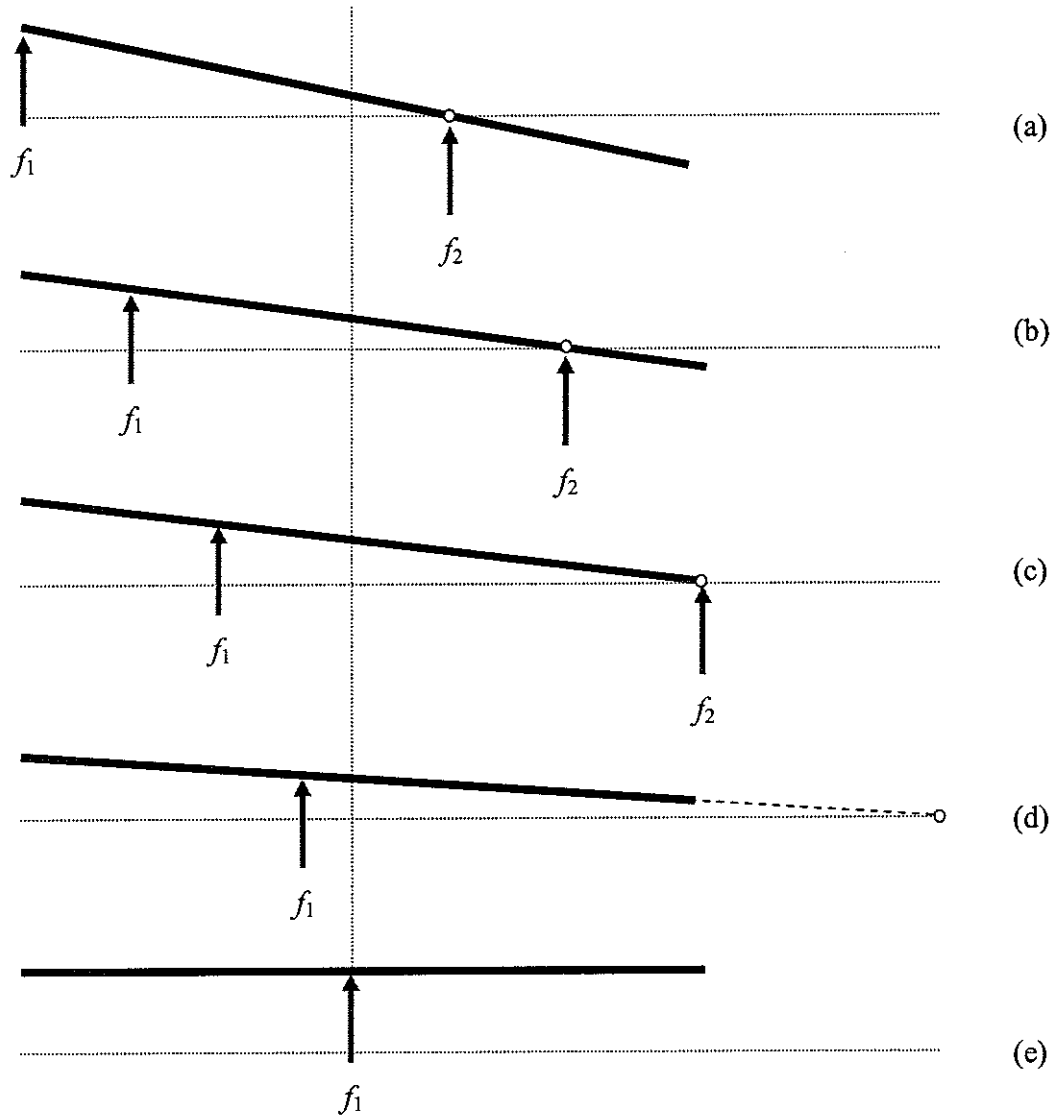

Figure 4.2 Some orientations of a rigid body beam showing points where the application of a secondary control force will not reduce the overall kinetic energy (a-c), and where the application of a secondary force anywhere on the beam will reduce the kinetic energy (d-e).

Figures 4.2 (a-c) all have a pivot point on the beam, about which the beam is rotating due to the application of the primary force. If the secondary control force were

applied at these points of rotation then the moment due to f_1 will not be cancelled. For figure 4.2d, the beam appears to rotate about a point off the end of the beam. A secondary force can be positioned anywhere on the beam in order to reduce the overall kinetic energy. For figure 4.2e the beam does not rotate, in this case the secondary force can be applied at any point on the beam in order to reduce the kinetic energy. In order to minimise the rigid body kinetic energy in the case of pure translation only, the secondary force would be equal in amplitude and 180 degrees out of phase with the primary force. In the specific case when the secondary force is coincident with the primary and is equal in amplitude and opposite phase then clearly the time averaged kinetic energy is zero. In general for practical machine installations, for example, the coincident case will never be achievable.

Figure 4.3 shows the full optimisation using equation (2.27) when the primary force is applied at the end and the secondary force at $\frac{2l}{3}$ as depicted in figure 4.2a.

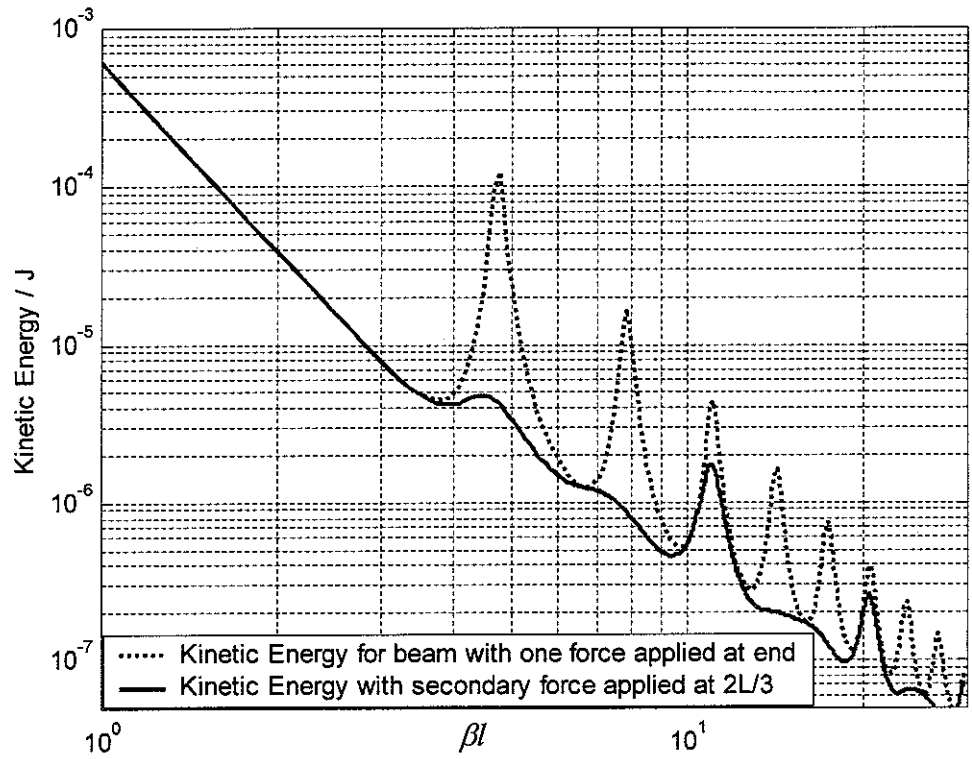

Figure 4.3 Total time averaged kinetic energy for a beam driven at one end by a single force, and for a beam with an additional secondary force at 2L/3. The magnitude and phase of the secondary force has been chosen to minimise the overall kinetic energy at each frequency

Figure 4.3 confirms the prediction of figure 4.2a and figure 4.1 that a secondary force in this position will not be effective in reducing the kinetic energy in the rigid body modes. As can be seen from figure 4.3, the minimisation has been effective for most of the flexural modes. Figure 4.4 depicts the cumulative energy in this case. Because a large proportion of the kinetic energy is in the rigid body modes, the minimisation has not been as effective as for the case depicted in figure 3.8.

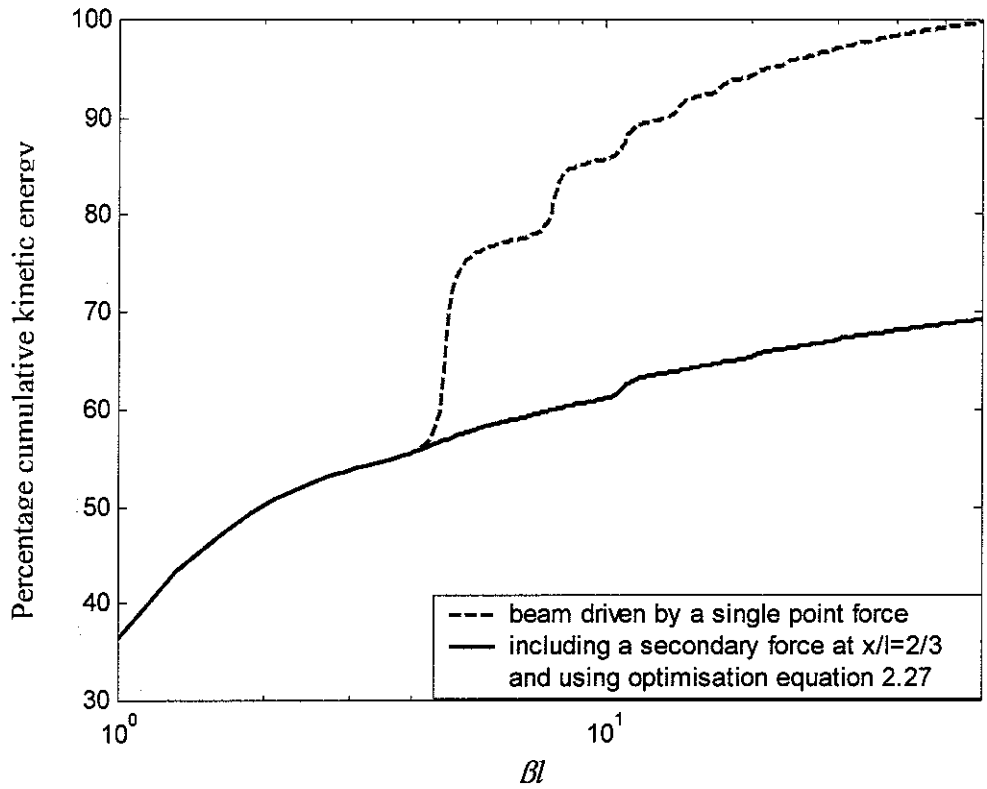

Figure 4.4 The cumulative time averaged kinetic energy as a percentage of the kinetic energy when the beam is driven by a single central point force (at x/l=0.5). a) for the beam driven by a single point force at the end, b) for the beam with a secondary force at x/l=2/3 and using the full minimisation equation (2.27) at each frequency.

5 Conclusions

Models have been developed to study how a thin elastic beam with free end conditions vibrates under the influence of two point forces. Two methodologies were utilised to calculate the time averaged kinetic energy of the beam. The first considers the beam as a continuous elastic structure and integrates the time averaged velocity along the length of the beam using a modal description. The second considers the beam as a series of lumped masses and sums the kinetic energy of each small mass element to determine the total time averaged kinetic energy. Both methods are in good agreement if the number of discrete mass elements per wavelength is greater than 5.

Both the modal and discretized models allow the Kinetic Energy to be formulated using the standard Hermitian quadratic form. For this form of the equation, methods exist for calculating the magnitude and phase of the second force in order to obtain a minimum in the time averaged kinetic energy of the beam. The Hermitian quadratic form was developed in a general form to allow for any number of secondary forces.

Two rigid body modes exist for a beam with free end conditions. These correspond to translation and rotation of the beam without bending. The models show that the rigid body modes can contribute a large proportion of the total kinetic energy for frequencies below the first flexural mode.

A simpler model was developed to minimise the kinetic energy in just the rigid body modes. The rigid body model was used to show that if the primary force is on either of the intervals $\left[0,\frac{l}{3}\right]$ or $\left[\frac{2l}{3},l\right]$ there is a position for the secondary force where the time averaged kinetic energy in the rigid body modes cannot be reduced. This position corresponds to the point about which the rigid beam is rotating when the single primary force is applied. If the primary force is on the interval $\frac{l}{3} < x_1 < \frac{2l}{3}$, then a secondary force of the correct amplitude and phase can always reduce the kinetic energy.

The optimum position for the secondary force is always co-located with the primary force. In which case, total cancellation can be achieved if the secondary force is of the same magnitude and 180 degrees out of phase.

6 References

1. Brennan, M.J., Elliott, S. J., and Pinnington, R. J., *Strategies for the active control of flexural vibration on a beam*, Journal of Sound and Vibration, **186**(4), 657-688, 1995.
2. Di Turo, P., *Feedforward control of vibrational kinetic energy of a beam using a piezoelectric actuator,* Communication with Prof. Brennan, 2003.
3. Gardonio, P. and Brennan, M. J., *Mobility and Impedance Methods in Structural Dynamics*, Chapter 9 in Fahy, F. J. and Walker, J. *Advanced Applications in Acoustics, Noise and Vibration,* 2004.
4. Gaudenzi, P., Carbonaro, R. and Benzi, E., *Control of beam vibrations by means of piezoelectric devices: theory and experiments*, Composite Structures, **50**, 373-379, 2000.
5. Halkyard, C. R., and Mace, B. R., *Feedforward adaptive control of flexural vibration in a beam using wave amplitudes*, Journal of Sound and Vibration, **254**(1), 117-141, 2002.
6. Nelson, P. and Elliott, S., *Active Control of Sound*, Academic Press, 1992.
7. Rao, S. S. Mechanical Vibrations Fourth Edition, Chapter 8, p612, *Continuous systems*, Prentice Hall, 2004.
8. Risi, J. D., Burdisso, R. A. and Fuller, C. R., *Analytical investigation of active control of radiated inlet fan noise*, J. Acoust. Soc. Am. **99**(1), 408-416,1996
9. Warburton, G.B. The Dynamical Behaviour of Structures (2nd Edition), Pergamon Press Ltd, 1976.